Hindawi
Mathematical Problems in Engineering
Volume 2020, Article ID 6661793, 11 pages
https://doi.org/10.1155/2020/6661793

Research Article

Memetic Salp Swarm Algorithm-Based Frequency Regulation for Power System with Renewable Energy Integration

Fang Zeng and Hongchun Shu

Faculty of Electric Power Engineering, Kunming University of Science and Technology, Kunming 650500, China

Correspondence should be addressed to Hongchun Shu; fanger1119@kust.edu.cn

Received 12 November 2020; Revised 25 November 2020; Accepted 29 November 2020; Published 14 December 2020

Academic Editor: Xiao-Shun Zhang

As the penetration of renewable energy to power grid increases gradually, to ensure the safety and stable operation of power system, it is necessary for renewable energy to participate in the secondary frequency regulation of power system. Therefore, this paper proposes an optimal control model of renewable energy participating in the secondary frequency regulation to solve the dynamic power distribution problem. Besides, memetic salp swarm algorithm (MSSA) is used to solve this complex nonlinear optimization problem, so as to quickly obtain high-quality power distribution schemes under different power perturbations and maximize the dynamic response regulation performance of the entire regional power grid. Finally, based on the improved IEEE standard two-area model, the established model is verified and the performance of the applied algorithm is tested by comparing the traditional engineering allocation method and other intelligent optimization algorithms.

1. Introduction

In recent years, to cope with climate change and sustainable energy development, the penetration of renewable energy connected to power grid has increased rapidly [1–3]. Different from traditional hydrothermal power, wind power and photovoltaic (PV) power with relatively mature technologies are greatly affected by meteorological conditions, so their power fluctuations are highly random [4–6]. As the regional power grid usually cannot fully absorb renewable energy such as wind or solar energy, it is easy to disconnect the wind farm or PV station from the power grid, which also greatly increases the pressure of frequency regulation of the system [7–10]. In this situation, the traditional configuration of hydropower plant and thermal power station as the main frequency regulation resources has been difficult to meet the high quality of the system's dynamic frequency regulation needs [11–13].

Therefore, the development of new high-quality frequency regulation resources has become one of the main means to relieve the pressure of regional power grid [14–16]. Compared with traditional hydropower plant and thermal power station, wind farm and PV station have faster response speed as well as climbing speed and rapid power fluctuations can be balanced more quickly [17–19]. Therefore, for regional power grids with high renewable energy penetration, especially in low-load areas, and wind farm, PV station can be used on power point control method to control it in below the operation condition of maximum power point, with a certain reserve capacity to participate in the secondary frequency regulation [6, 20, 21], called automatic generation control (AGC) [22–24].

In general, AGC mainly consists of two parts [25–27]: (1) based on the real-time acquisition of frequency and power deviation of the tie line, a centralized controller, such as proportional-integral (PI) controller, is used to acquire the approximate actual power fluctuation of the system, and then the total power instruction of the regional power network is issued; (2) according to the power allocation algorithms, the total power instruction is assigned to each unit participating in the frequency regulation [28–30]. Literature [31] proposes a sliding mode controller for multisource AGC system using teaching and learning-based optimization algorithm. Literature [32] proposes a lifelong learning-based complementary generation control of power grids with renewable energy sources. Literature [33] proposes AGC of a multiarea multisource hydrothermal power system. However, although the abovementioned literature realizes the control of multisource participating in AGC, the modeling is relatively simple, considering only the climbing response characteristics of the units and not other dynamic response characteristics of different frequency regulation resources, which will affect the overall control effect of the system and easily make the system deviate greatly from the optimal operating point. Therefore, this paper proposes a multisource optimal collaborative control method for wind and solar renewable energy based on its dynamic response characteristics to participate in secondary frequency regulation.

In essence, AGC optimal control is a complex nonlinear optimization problem [34–36]. In practice, power distribution is often not optimized but arranged according to adjustable capacity ratio and climbing speed, which cannot meet the optimal control requirements of the system [37–40]. On the other hand, traditional mathematical optimization methods (such as interior point method [41]), although fast in solving problems, have poor global searching ability and are prone to fall into local optimal solutions. In comparison, genetic algorithm (GA) [42–44] and other metaheuristic algorithms [45–47] have higher application flexibility and better global search capability, but their solving speed is slow and cannot meet the needs of AGC online control for large-scale regional power grids [48–50]. Therefore, MSSA with a faster convergence speed is used to solve the problem. Compared with the original salp swarm algorithm (SSA), memetic salp swarm algorithm (MSSA) employs multiple independent slap chains to simultaneously implement the exploration and exploitation [51]. Besides, MSSA also has low dependence on the mathematical model. To verify the validity of the proposed method, this paper used the improved IEEE standard two-area model for simulation test and analysis.

The remaining of this paper is organized as follows: Section 2 develops the optimal control model for automatic generation control. In Section 3, MSSA is described. Comprehensive case studies are undertaken in Section 4. Section 5 summarizes the main contributions of the paper.

2. Optimal Control Model for Automatic Generation Control

2.1. Control Framework. Generally, AGC has the following three control modes: (a) flat frequency control, (b) flat tie-line control, and (c) tie-line bias control. Also, tie-line bias control was used in this paper. The two-region interconnection power network is depicted in Figure 1, in which the AGC control process of each region includes two parts: controller control and optimal power distribution. A PI controller is adopted to convert the power deviation and frequency deviation of the real-time receiving tie line into regional control deviation as input and output to the real-time adjusting power of the regional power grid ΔP. Then, ΔP is assigned to each AGC unit through the power allocation algorithm. Different from the traditional power system with hydropower plant and thermal power station as the main reserve capacity, wind farm and PV station no longer need to be disconnected from the grid but participate in the power AGC regulation of the system.

2.2. Dynamic Response Model of Units. The establishment of dynamic response model of the units is mainly in order to more accurately describe the units after the received power adjusts instruction power dynamic response process. For different types of units, the dynamic response model not only regulates the upper and lower limits of capacity, climbing rate, frequency regulation delay, and other common parts [52] but also includes transmission links with their own energy conversion characteristics. Besides, AGC often uses the frequency domain model to describe the dynamic response process of the units, as shown in Figure 2. T_d represents the secondary frequency regulation delay of the units; $G(s)$ represents the power response transfer function of the units, as shown in Table 1. $T_1 \sim T_9$ are the known parameters of the transfer function, respectively [53]. Therefore, according to the inverse Laplace transform of the frequency domain transfer function, the real-time output of the regulated power can be calculated through the input power, as follows:

$$\Delta P_i^{\text{out}}(t) = L^{-1}\left\{\frac{G_i(s)}{s\left(1+T_d^i s\right)} \cdot \sum_{k=1}^{N}\left[e^{-\Delta T\cdot(k-1)s} \cdot D_i^{\text{in}}(k)\right]\right\}, \tag{1}$$

$$D_i^{\text{in}}(k) = \Delta P_i^{\text{in}}(k) - \Delta P_i^{\text{in}}(k-1), \tag{2}$$

$$\Delta P_i^{\text{out}}(k) = \Delta P_i^{\text{out}}(t = k\cdot\Delta T), \tag{3}$$

where i represents the i^{th} AGC unit; K represents the k^{th} discrete control period; ΔP_i^{in} and ΔP_i^{out} represent the input regulation power command and real-time output of regulated power of the i^{th} AGC unit, respectively; and ΔT represents the control period of AGC, with a value of 1 to 16 seconds.

2.3. Optimization Mathematical Model. A performance index is assigned to quantify the total power response deviation, which is defined as the sum of the absolute deviation value of the regulating power command value and the power output value of all units, as follows:

$$\min f = \sum_{j=k}^{N}\sum_{i=1}^{n}\left|\Delta P_i^{\text{in}}(j) - \Delta P_i^{\text{out}}(j)\right|, \tag{4}$$

where N represents the number of control periods and n represents the number of AGC units.

In addition to considering the dynamic response transfer process of the units, some constraint conditions, such as power balance constraint, units capacity constraint, and

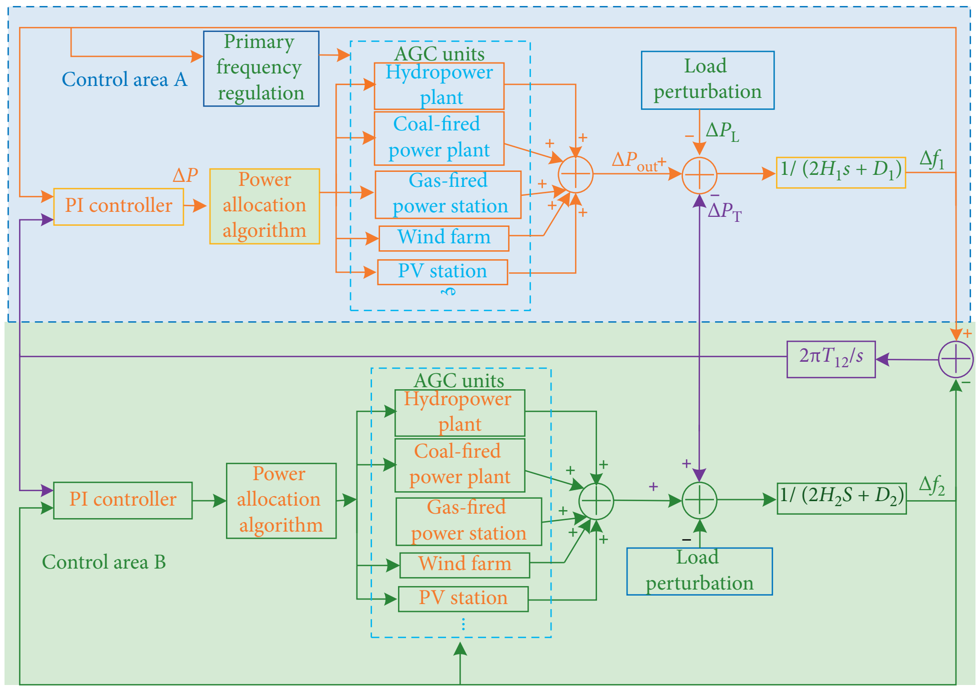

Figure 1: Illustration of coordinated control of multisource for AGC under two-area framework.

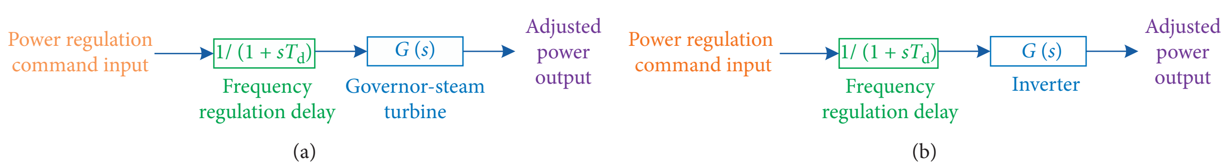

Figure 2: Dynamic response models of different types of AGC units. (a) Traditional hydropower plant and thermal power station. (b) Wind farm and PV station.

climbing constraint, should also be considered in the power distribution process, as follows:

$$\Delta P^{\mathrm{in}}(k)=\sum_{i=1}^{n}\Delta P_i^{\mathrm{in}}(k), \tag{5}$$

$$\Delta P^{\mathrm{in}}(k)\cdot\Delta P_i^{\mathrm{in}}(k)\geq 0,\quad i=1,2,\ldots,n, \tag{6}$$

$$\Delta P_i^{\min}\leq\Delta P_i^{\mathrm{in}}(k)\leq\Delta P_i^{\max},\quad i=1,2,\ldots,n, \tag{7}$$

$$\left|\Delta P_i^{\mathrm{in}}(k)-\Delta P_i^{\mathrm{in}}(k-1)\right|\leq\Delta P_i^{\mathrm{rate}},\quad i=1,2,\ldots,n, \tag{8}$$

where ΔP^{in} represents total power regulation command and $\Delta P_i^{\mathrm{rate}}$ represents the maximum climbing speed of the i^{th} AGC units.

3. Memetic Salp Swarm Algorithm

3.1. Inspiration. Salps are marine creatures that resemble jellyfish in body structure and movement. They are usually joined end to end to form a chain, also known as a salp chain. The leader is located at the first end of the chain and has the best judgment of environment and food source. The remaining salps are followers, who follow the previous one in turn. This movement mode is conducive to the rapid coordinated movement and feeding of the salps group. Literature [54] established a mathematical model of salps chain in 2017 and proposed SSA to solve a series of optimization problems.

3.2. Optimization Framework. This paper is combined with cultural genetic algorithm, aiming at the shortcomings of SSA algorithm to improve, and defined as MSSA. The optimization process is as follows: the culture of each salp is defined as a solution to the optimization problem. All salps in the community are divided into different populations in the unit of salp chain, and each salp chain has its own culture and independently searches for food sources. At the same time, the culture of each salp affects and is influenced by other individuals and evolves with the evolution of the population. When the population evolution reaches a certain stage, the whole community will exchange information to realize the mixed evolution of the population until the convergence condition of the optimization problem is satisfied.

The optimization framework of MSSA is shown in Figure 3, which mainly includes the following two operations, as follows [54]:

Table 1: Dynamic response transfer functions of different AGC units.

Type	Transfer function
Nonreheat turbine	$1/1+T_1 s$
Reheat turbine	$(1+T_2 s/(1+T_3 s)(1+T_4 s)(1+T_5 s))$
Hydropower	$((1-T_6 s)(1+T_7 s)/(1+0.5T_6 s)(1+T_8 s))$
Wind and solar renewable energy	$1/1+T_9 s$

(a) Local search in each chain: each salp chain will implement a local search to improve the ability of global exploration and local exploitation;

(b) Global coordination in virtual population: each salp is taken as a virtual population, and the population will be regrouped into multiple new salp chains. Hence, a global coordination can be achieved.

3.3. Local Search in Each Chain. The salp chain can be divided into two roles, i.e., the leader and the follower. It is worth noting that the leader is responsible for directing the entire salp chain to the food source, following each other. For the m^{th} salp chain, the position of the leader can be updated, as follows [55]:

$$x_{m1}^{j}=\begin{cases}F_m^j+c_1\left(c_2\left(ub^j-lb^j\right)+lb^j\right), & c_3\geq 0,\\ F_m^j-c_1\left(c_2\left(ub^j-lb^j\right)+lb^j\right), & c_3<0,\end{cases}\tag{9}$$

where the superscript j represents the j^{th} dimension of the searching space; x_{mi}^{j} is the position of the leader in the m^{th} salp chain; F_m^j denotes the position of the food source, i.e., the current best solution obtained by the m^{th} salp chain; and u_b^j and l_b^j are the upper and lower bounds of the j^{th} dimension, respectively; $c_1=2e^{-(4k/k_{\max})^2}$, where k is the current iteration number and $k_{\max}$ is the maximum iteration number, respectively. Besides, c_2 and c_3 are the random numbers, respectively, and $c_2, c_3\in[0,1]$ [56].

In addition, the position of the followers can be updated, as follows [55]:

$$x_{mi}^{j}=\frac{1}{2}\left(x_{mi}^{j}+x_{m,i-1}^{j}\right),\quad i=2,3,\ldots,n, m=1,2,\ldots,M,\tag{10}$$

where x_{mi}^{j} is the position of the i^{th} salp in the m^{th} salp chain; n is the population size of each salp chain; and M is the number of salp chains, respectively.

3.4. Global Coordination in Virtual Population. To achieve a global coordination, the virtual population will be regrouped into different salp chains according to the salps' fitness values, as shown in Figure 4. Specifically, all salps are sorted according to the order of fitness from large to small. Finally, the salps will be divided into M^{th} salp chains, and the distribution rules are as follows: the first salp regroups into the first chain, the M^{th} salps into the M^{th} chain, the $M+1^{\text{th}}$ into the first chain, and so on. The update rules of the M^{th} salp chain are described as follows [57]:

$$Y^m=\left[x_{mi}, f_{mi}|x_{mi}=X(m+M(i-1)), f_{mi}=F(m+M(i-1)),\quad i=1,2,\ldots,n\right], m=1,2,\ldots,M,\tag{11}$$

where x_{mi}^{j} is the position vector of the i^{th} salp in the m^{th} chain; f_{mi} is the fitness value of the i^{th} salp in the m^{th} chain; F is the fitness value set of all the salps following the descending order; and X is the corresponding position vector set of all the salps, i.e., a position matrix, as follows:

$$X=\begin{bmatrix}x_1^1 & x_1^2 & \cdots & x_1^d\\ x_2^1 & x_2^2 & \cdots & x_2^d\\ \vdots & \vdots & \ddots & \vdots\\ x_{n\times M}^1 & x_{n\times M}^2 & \cdots & x_{n\times M}^d\end{bmatrix},\tag{12}$$

where d is the number of dimensions, and each row vector represents the position vector of each salp.

In addition, the overall flowchart of MSSA is given in Figure 5.

3.5. MSSA Design for AGC System. In order to ensure that the initial solution is a feasible solution, this paper forms the initial solution according to an engineering method called PROP method. In other words, the initial solution is obtained by the same adjustable capacities' ratio.

On the other hand, this paper applies the penalty function method to the fitness function $\text{Fit}(x)$ to satisfy the constraint conditions (5)–(8), as follows:

$$\text{Fit}(x)=\begin{cases}f(x), & \text{if constraints are satisfied},\\ f(x)+M\left(Z_u-Z_u^{\lim}\right)^2, & \text{otherwise},\end{cases}\tag{13}$$

where M is the penalty function factor, and its value is usually a relatively large positive number; Z_u is the u^{th} constraint; and $Z_u^{\lim}$ is the limit of the u^{th} constraint.

4. Case Studies

The proposed methodology is tested on the IEEE load frequency control model. It is worth noting that 1 AGC unit in region A is increased to 5 units, as shown in Figure 1. Besides, Tables 2 and 3 show the main parameters of response transfer and power regulation of the units, respectively, and the control period of AGC is set to 4 seconds. Also, the response performance is compared to that of PROP, GA, and SSA. To achieve a fair comparison, the population size is set to 10 and the maximum number of

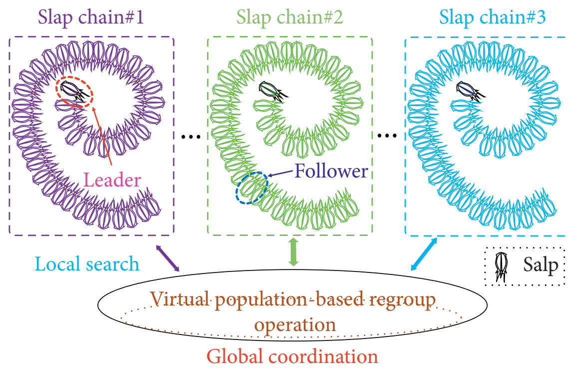

FIGURE 3: Optimization framework of MSSA.

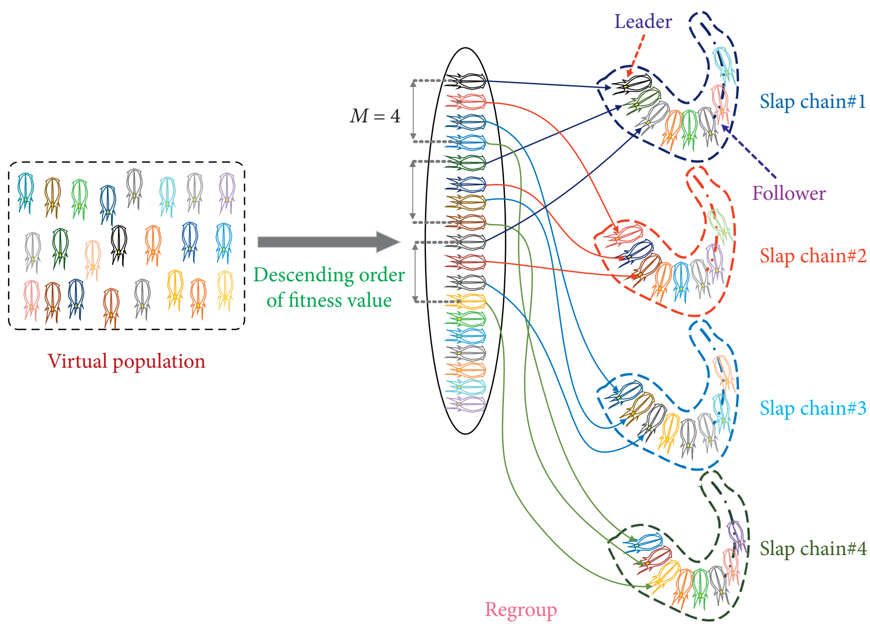

FIGURE 4: Regroup operation of virtual population.

iterations is set to 100. It is worth noting that if the parameters are not chosen properly, the convergence time will be too long or the local optimum will be trapped. Besides, ode23 was selected as the solver, and the sampling rate was set to 0.001 s.

4.1. Convergence Research. Figure 6 shows the convergence curves of MSSA under different power distribution instructions. It can be found that MSSA can solve the optimal solution with high quality after 30 steps of iteration, and the subsequent iteration only makes slight reduction adjustment, which also indicated the fast convergence of the algorithm. In order to better evaluate the quality of the optimal solution of different methods, Table 4 shows the comparison of the convergence results of different methods, in which each indicator unit is MW. It shows that PROP performs power allocation according to the ratio of the adjustable capacity of the unit, so the power output of thermal power units with larger regulating capacity is relatively high, and it will lead to a large power deviation. On the other hand, GA, SSA, and MSSA can significantly reduce power deviation after their respective optimization operation, and MSSA has the best performance.

4.2. Online Optimization. In order to evaluate the online optimization performance of MSSA, in the area of A, a step power perturbation $\Delta P_L = 80$ MW has occurred. The online optimization results of MSSA and PROP are compared as shown in Figure 7. Compared with previous optimization, the power deviation obtained by MSSA is smaller, and the overshoot of the total power instruction can be avoided. In addition, wind farm and PV station can recover the power system disturbed by high power quickly in the initial stage of power disturbance because of their fast response speed.

To further test the optimization performance of different algorithms, Table 5 presents the online optimization results of different algorithms (the optimal value is marked in bold), in which area control error (ACE), $|\Delta f_1|$, and CPS1 are the average values in the simulation. Besides, the power deviation is the total deviation in the simulation

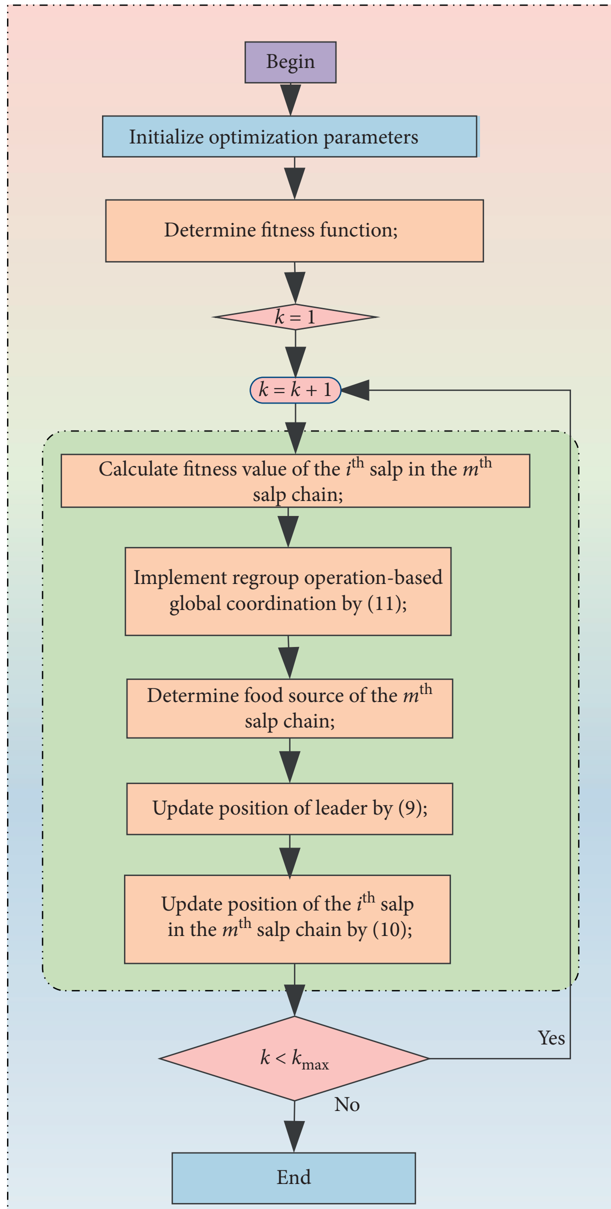

Figure 5: The general procedure of MSSA.

Table 2: Parameters of dynamic response transfer functions of AGC units.

Units	Type	Parameters of transfer function
G_1	Thermal power station	$T_2 = 5,\ T_3 = 0.08,\ T_4 = 10,\ T_5 = 0.3$
G_2	LNG units	$T_2 = 2,\ T_3 = 0.05,\ T_4 = 5,\ T_5 = 0.2$
G_3	Hydropower plant	$T_6 = 1,\ T_7 = 5,\ T_8 = 0.513$
G_4	Wind farm	$T_1 = 0.01$
G_5	PV station	$T_1 = 0.01$

time. Accuracy is used to measure the fitting degree of the actual adjustment output and the adjustment instruction curve in the simulation time. It can be found that, compared with PROP, the other three methods can significantly reduce power deviation, thus significantly improving the system's dynamic response performance. Compared with GA and SSA, the online optimization results of MSSA are better, which is because memetic computing framework can observably improve the ability of exploration and exploitation.

Table 3: Main parameters of power regulation of AGC units.

Units	T_d (s)	ΔP^{rate} (MW/min)	ΔP^{max} (MW)	ΔP^{min} (MW)
G_1	60	30	50	−50
G_2	20	18	30	−30
G_3	5	150	20	−10
G_4	1	—	15	−5
G_5	1	—	10	−10

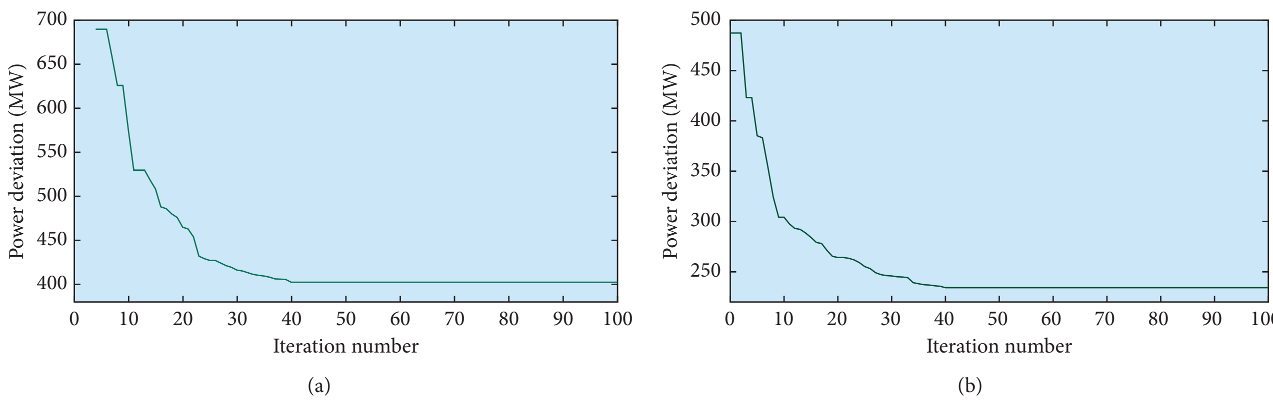

Figure 6: Convergence curves of MSSA. (a) $\Delta P_{in} = 80$ MW. (b) $\Delta P_{in} = -50$ MW.

Table 4: Comparison on convergence results obtained by different methods.

ΔP^{in}	Method	ΔP_1^{in}	ΔP_2^{in}	ΔP_3^{in}	ΔP_4^{in}	ΔP_5^{in}	Power deviation
80	PROP	32.00	19.20	12.80	9.60	6.40	676.95
	GA	15.52	23.18	17.92	12.7	10.68	529.86
	SSA	10.61	25.74	17.26	14.67	11.72	471.48
	MSSA	14.26	20.84	19.52	15.12	10.26	402.451
−50	PROP	−23.81	−14.29	−4.76	−2.38	−4.76	479.83
	GA	−4.26	−23.24	−10.02	−3.86	−8.62	274.26
	SSA	−8.65	−20.62	−9.85	−4.29	−6.59	307.48
	MSSA	−4.48	−20.69	−9.14	−5.58	−10.11	234.254

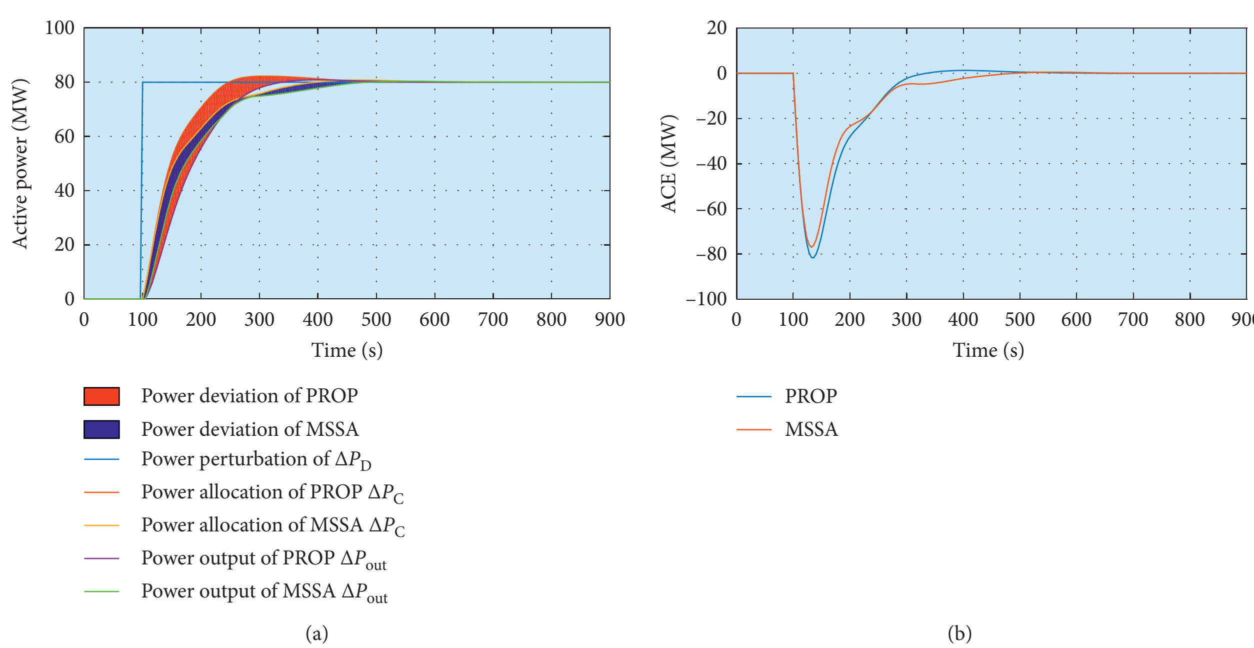

Figure 7: Continued.

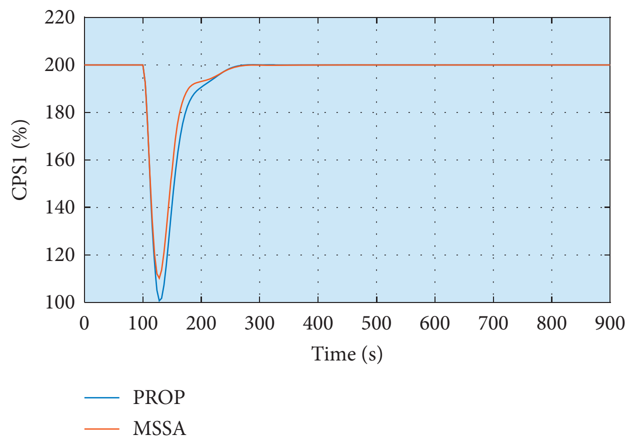

(c)

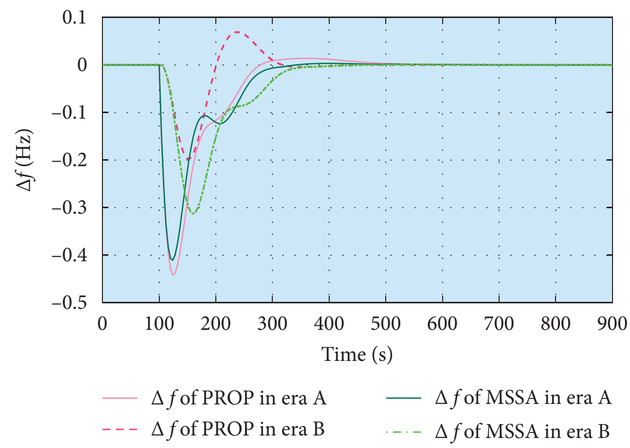

(d)

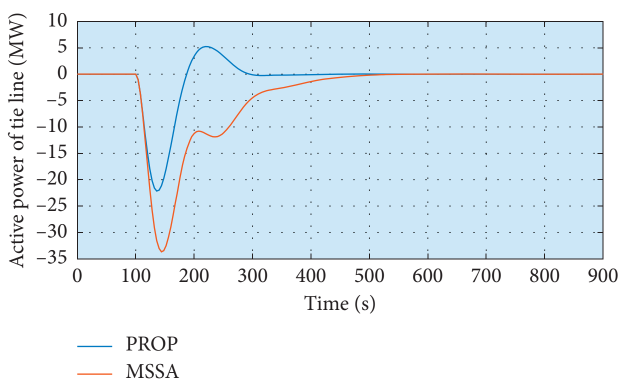

(e)

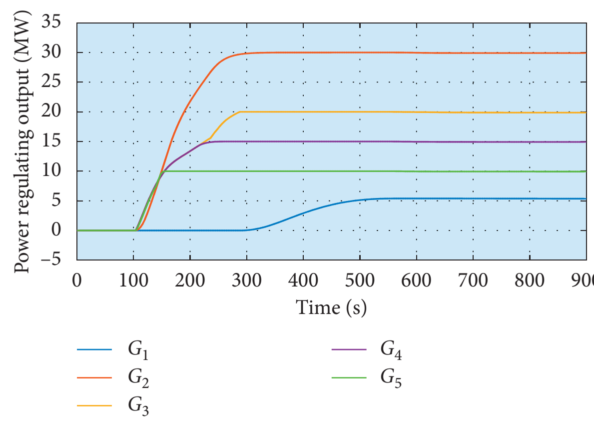

(f)

Figure 7: Result comparison of online optimization by MSSA and without optimization when $\Delta P_L = 80$ MW. (a) Total power regulation curve. (b) Curve of ACE. (c) Curve of CPS1. (d) Frequency deviation Δf. (e) Active power of tie line (MW). (f) Power output curve of the units.

Table 5: Result comparison of online optimization obtained by different methods.

ΔP_L	Algorithms	|ACE| (MW)	Δf_1 (Hz)	CPS1 (%)	Accuracy (%)	Power deviation (MW)
80	PROP	7.7678	0.0356	194.69	95.84	630.05
	GA	7.4209	0.0323	195.86	98.25	261.32
	SSA	7.5095	0.0321	195.84	98.17	267.52
	MSSA	7.3995	0.0316	195.57	98.84	254.21
−50	PROP	5.0541	0.0235	197.78	94.99	477.46
	GA	4.6046	0.0203	198.25	98.21	164.26
	SSA	4.6044	0.0202	198.29	98.23	161.48
	MSSA	4.6040	0.0196	198.36	98.41	149.96

5. Conclusions

In this paper, a multisource optimal collaborative control method for power system with renewable energy participation in secondary frequency regulation is proposed. The main contributions can be summarized as follows:

(i) A novel AGC control model is established for the power system with high renewable energy penetration to improve the dynamic response performance of the system;

(ii) The study verified the effectiveness of MSSA for AGC. It can not only meet the online regulation requirements of AGC but also quickly obtain high-quality regulation schemes with high convergence stability, and the dynamic response performance of the entire regional power grid is significantly improved.

Besides, electric vehicles will be considered to participate in AGC in future studies.

Abbreviations

ΔP_i^{in}: Input regulation power command of the i^{th} AGC unit
ΔP_i^{out}: Real-time output of regulated power of the i^{th} AGC unit
ΔT: Control period of AGC
N: Number of control periods
n: Number of AGC units
ΔP_i^{rate}: Maximum climbing speed of the i^{th} AGC units
x_{mi}^j: Position of the leader in the m^{th} salp chain
F_m^j: Position of the food source
x_{mi}^j: Position vector of the i^{th} salp in the m^{th} chain
f_{mi}: Fitness value of the i^{th} salp in the m^{th} chain
F: Fitness value set of all the salps following the descending order
X: Corresponding position vector set of all the salps
PV: Photovoltaic
AGC: Automatic generation control
GA: Genetic algorithm
SSA: Salp swarm algorithm
MSSA: Memetic salp swarm algorithm.

Data Availability

The data that support the findings of this study are available upon request from the corresponding author. The data are not publicly available due to privacy or ethical restrictions.

Conflicts of Interest

The authors declare no conflicts of interest.

Acknowledgments

The authors gratefully acknowledge the support of the National Natural Fund of China (52037003) and Key Science and Technology Project of Yunnan Province (202002AF080001).

References

[1] B. Yang, L. Jiang, L. Wang, W. Yao, and Q. H. Wu, "Nonlinear maximum power point tracking control and modal analysis of DFIG based wind turbine," *International Journal of Electrical Power & Energy Systems*, vol. 74, pp. 429–436, 2016.
[2] B. Yang, T. Yu, X. Zhang et al., "Dynamic leader based collective intelligence for maximum power point tracking of PV systems affected by partial shading condition," *Energy Conversion and Management*, vol. 179, pp. 286–303, 2019.
[3] B. Yang, T. Yu, H. Shu et al., "Passivity-based sliding-mode control design for optimal power extraction of a PMSG based variable speed wind turbine," *Renewable Energy*, vol. 119, pp. 577–589, 2018.
[4] X. Zhang, T. Yu, B. Yang, and L. Li, "Virtual generation tribe based robust collaborative consensus algorithm for dynamic generation command dispatch optimization of smart grid," *Energy*, vol. 101, pp. 34–51, 2016.
[5] Z. Wang, J. Zhong, and J. Li, "Design of performance-based frequency regulation market and its implementations in real-time operation," *International Journal of Electrical Power & Energy Systems*, vol. 87, pp. 187–197, 2017.
[6] L. R. Chang-Chien, C. C. Sun, and Y. J. Yeh, "Modeling of wind farm participation in AGC," *IEEE Transactions on Power Systems*, vol. 29, no. 3, pp. 1204–1211, 2013.
[7] J. M. Morales, L. Baringo, A. J. Conejo, and R. Mínguez, "Probabilistic power flow with correlated wind sources," *IET Generation, Transmission & Distribution*, vol. 4, no. 5, pp. 641–651, 2010.
[8] M. Sun, H. Wu, Y. Qiu, and Y. Song, "Probability load flow for wind power integrated system based on generalized polynomial chaos method," *Automation of Electric Power Systems*, vol. 41, no. 7, pp. 54–60, 2017.
[9] B. R. Prusty and D. Jena, "A critical review on probabilistic load flow studies in uncertainty constrained power systems with photovoltaic generation and a new approach," *Renewable and Sustainable Energy Reviews*, vol. 69, pp. 1286–1302, 2017.
[10] V. Lakshmanan, M. Marinelli, J. Hu, and H. W. Bindner, "Provision of secondary frequency control via demand response activation on thermostatically controlled loads: solutions and experiences from Denmark," *Applied Energy*, vol. 173, pp. 470–480, 2016.
[11] R. Fantino, J. Solsona, and C. Busada, "Nonlinear observer-based control for PMSG wind turbine," *Energy*, vol. 113, pp. 248–257, 2016.
[12] L. Dong, W. Cheng, and Y. Yang, "Probabilistic load flow calculation for power grid containing wind farms," *Power System Technology*, vol. 16, pp. 87–91, 2009.
[13] B. Yang, L. Jiang, W. Yao, and Q. H. Wu, "Perturbation estimation based coordinated adaptive passive control for multimachine power systems," *Control Engineering Practice*, vol. 44, pp. 172–192, 2015.
[14] B. Yang, J. Wang, X. Zhang et al., "Comprehensive overview of meta-heuristic algorithm applications on PV cell parameter identification," *Energy Conversion and Management*, vol. 208, Article ID 112595, 2020.
[15] M. S. Ćalović, "Advanced automatic generation control with automatic compensation of tie-line losses," *Electric Power Components and Systems*, vol. 40, no. 7, pp. 807–828, 2012.
[16] X. Zhao, Z. Lin, B. Fu, L. He, and N. Fang, "Research on automatic generation control with wind power participation based on predictive optimal 2-degree-of-freedom PID strategy for multi-area interconnected power system," *Energies*, vol. 11, no. 12, p. 3325, 2018.
[17] B. Yang, X. Zhang, T. Yu, H. Shu, and Z. Fang, "Grouped grey wolf optimizer for maximum power point tracking of doubly-fed induction generator based wind turbine," *Energy Conversion and Management*, vol. 133, pp. 427–443, 2017.
[18] G. Rashid and M. H. Ali, "Nonlinear control-based modified BFCL for LVRT capacity enhancement of DFIG-based wind farm," *IEEE Transactions on Energy Conversion*, vol. 32, no. 1, pp. 284–295, 2016.
[19] N. H. Saad, A. A. Sattar, and A. E.-A. M. Mansour, "Low voltage ride through of doubly-fed induction generator connected to the grid using sliding mode control strategy," *Renewable Energy*, vol. 80, pp. 583–594, 2015.
[20] B. Yang, T. Yu, H. Shu, J. Dong, and L. Jiang, "Robust sliding-mode control of wind energy conversion systems for optimal power extraction via nonlinear perturbation observers," *Applied Energy*, vol. 210, pp. 711–723, 2018.
[21] P. P. Zarina, S. Mishra, and P. C. Sekhar, "Exploring frequency control capability of a PV system in a hybrid PV-rotating

machine-without storage system," *International Journal of Electrical Power & Energy Systems*, vol. 60, pp. 258–267, 2014.

[22] G. Sharma, I. Nasiruddin, and K. R. Niazi, "Optimal automatic generation control of asynchronous power systems using output feedback control strategy with dynamic participation of wind turbines," *Electric Power Components and Systems*, vol. 43, no. 4, pp. 384–398, 2015.

[23] X. Zhang, T. Yu, B. Yang, L. Zheng, and L. Huang, "Approximate ideal multi-objective solution $Q(\lambda)$ learning for optimal carbon-energy combined-flow in multi-energy power systems," *Energy Conversion and Management*, vol. 106, pp. 543–556, 2015.

[24] C. Zhang, J. Chen, M. Liu et al., "Regulation mechanism of biomolecule interaction behaviors on the superlubricity of hydrophilic polymer coatings," *Protection and Control of Modern Power Systems*, 2020.

[25] A. G. Pillai, E. R. Samuel, and A. Unnikrishnan, "Minimal realized power systems for load frequency control using optimal theory based PID controller," *IETE Journal of Research*, vol. 5, no. 1, pp. 1–13, 2020.

[26] J. Liu, W. Yao, J. Wen et al., "Impact of power grid strength and PLL parameters on stability of grid-connected DFIG wind farm," *IEEE Transactions on Sustainable Energy*, vol. 11, no. 1, pp. 545–557, 2020.

[27] D. Song, X. Fan, J. Yang, A. Liu, S. Chen, and Y. H. Joo, "Power extraction efficiency optimization of horizontal-axis wind turbines through optimizing control parameters of yaw control systems using an intelligent method," *Applied Energy*, vol. 224, pp. 267–279, 2018.

[28] X. Zhang, Z. Xu, T. Yu, B. Yang, and H. Wang, "Optimal mileage based AGC dispatch of a GenCo," *IEEE Transactions on Power Systems*, vol. 35, no. 4, pp. 2516–2526, 2020.

[29] X. S. Zhang, T. Tan, B. Zhou, T. Yu, B. Yang, and X. M. Huang, "Adaptive distributed auction-based algorithm for optimal mileage based AGC dispatch with high participation of renewable energy," *International Journal of Electrical Power & Energy Systems*, vol. 124, Article ID 106371, 2020.

[30] Y. Shen, W. Yao, J. Wen, H. He, and L. Jiang, "Resilient wide-area damping control using GrHDP to tolerate communication failures," *IEEE Transactions on Smart Grid*, vol. 10, no. 3, pp. 2547–2557, 2019.

[31] B. Mohanty, "TLBO optimized sliding mode controller for multi-area multi-source nonlinear interconnected AGC system," *International Journal of Electrical Power & Energy Systems*, vol. 73, pp. 872–881, 2015.

[32] X. S. Zhang, T. Yu, Z. N. Pan, B. Yang, and T. Bao, "Lifelong learning for complementary generation control of interconnected power grids with high-penetration renewables and EVs," *IEEE Transactions on Power Systems*, vol. 33, no. 4, pp. 4097–4110, 2018.

[33] X. S. Zhang, Q. Li, T. Yu, and B. Yang, "Consensus transfer Q-learning for decentralized generation command dispatch based on virtual generation tribe," *IEEE Transactions on Smart Grid*, vol. 9, no. 3, pp. 2152–2165, 2018.

[34] M. Tan, C. J. Han, C. Han, X. Zhang, L. Guo, and T. Yu, "Hierarchically correlated equilibrium Q-learning for multi-area decentralized collaborative reactive power Optimization," *CSEE Journal of Power and Energy Systems*, vol. 2, no. 3, pp. 65–72, 2016.

[35] D. R. Song, S. Y. Zheng, S. Yang et al., "Annual energy production estimation for variable-speed wind turbine at high-altitude site," *Journal of Modern Power Systems and Clean Energy*, 2020.

[36] X. Peng, W. Yao, C. Yan, J. Wen, and S. Cheng, "Two-stage variable proportion coefficient based frequency support of grid-connected DFIG-WTs," *IEEE Transactions on Power Systems*, vol. 35, no. 2, pp. 962–974, 2020.

[37] X. He, L. Chu, R. C. Qiu, Q. Ai, Z. Ling, and J. Zhang, "Invisible units detection and estimation based on random matrix theory," *IEEE Transactions on Power Systems*, vol. 35, no. 3, pp. 1846–1855, 2019.

[38] X. Zhang, T. Yu, B. Yang, and L. Cheng, "Accelerating bio-inspired optimizer with transfer reinforcement learning for reactive power optimization," *Knowledge-Based Systems*, vol. 116, pp. 26–38, 2017.

[39] Y. Arya and N. Kumar, "AGC of a multi-area multi-source hydrothermal power system interconnected via AC/DC parallel links under deregulated environment," *International Journal of Electrical Power & Energy Systems*, vol. 75, pp. 127–138, 2016.

[40] A. S. El-Bakry, R. A. Tapia, T. Tsuchiya, and Y. Zhang, "On the formulation and theory of the Newton interior-point method for nonlinear programming," *Journal of Optimization Theory and Applications*, vol. 89, no. 3, pp. 507–541, 1996.

[41] S. P. Ghoshal, "Application of GA/GA-SA based fuzzy automatic generation control of a multi-area thermal generating system," *Electric Power Systems Research*, vol. 70, no. 2, pp. 115–127, 2004.

[42] A. Demiroren and H. L. Zeynelgil, "GA application to optimization of AGC in three-area power system after deregulation," *International Journal of Electrical Power & Energy Systems*, vol. 29, no. 3, pp. 230–240, 2007.

[43] T. Yu, X. S. Zhang, B. Zhou, and K. W. Chan, "Hierarchical correlated Q-learning for multi-layer optimal generation command dispatch," *International Journal of Electrical Power & Energy Systems*, vol. 78, pp. 1–12, 2016.

[44] X. Zhang, B. Yang, T. Yu, and L. Jiang, "Dynamic Surrogate Model based optimization for MPPT of centralized thermoelectric generation systems under heterogeneous temperature difference," *IEEE Transactions on Energy Conversion*, vol. 35, no. 2, pp. 966–976, 2020.

[45] X. Zhang, S. Li, T. He et al., "Memetic reinforcement learning based maximum power point tracking design for PV systems under partial shading condition," *Energy*, vol. 174, pp. 1079–1090, 2019.

[46] H. Golpîra, H. Bevrani, and H. Golpîra, "Application of GA optimization for automatic generation control design in an interconnected power system," *Energy Conversion and Management*, vol. 52, no. 5, pp. 2247–2255, 2011.

[47] R. K. Sahu, S. Panda, and G. T. Chandra Sekhar, "A novel hybrid PSO-PS optimized fuzzy PI controller for AGC in multi area interconnected power systems," *International Journal of Electrical Power & Energy Systems*, vol. 64, pp. 880–893, 2015.

[48] S. Panda, B. Mohanty, and P. K. Hota, "Hybrid BFOA-PSO algorithm for automatic generation control of linear and nonlinear interconnected power systems," *Applied Soft Computing*, vol. 13, no. 12, pp. 4718–4730, 2013.

[49] A. K. Barisal and S. Mishra, "Improved PSO based automatic generation control of multi-source nonlinear power systems interconnected by AC/DC links," *Cogent Engineering*, vol. 5, no. 1, Article ID 1422228, 2018.

[50] X. He, Q. Ai, R. C. Qiu, W. Huang, L. Piao, and H. Liu, "A big data architecture design for smart grids based on random matrix theory," *IEEE Transactions on Smart Grid*, vol. 8, no. 2, pp. 674–686, 2015.

[51] B. Yang, L. Zhong, X. Zhang et al., "Novel bio-inspired memetic salp swarm algorithm and application to MPPT for PV systems considering partial shading condition," *Journal of Cleaner Production*, vol. 215, pp. 1203–1222, 2019.

[52] T. Yu, Y. M. Wang, W. J. Ye, B. Zhou, and K. W. Chan, "Stochastic optimal generation command dispatch based on improved hierarchical reinforcement learning approach," *IET Generation, Transmission & Distribution*, vol. 5, no. 8, pp. 789–797, 2011.

[53] M. Datta and T. Senjyu, "Fuzzy control of distributed PV inverters/energy storage systems/electric vehicles for frequency regulation in a large power system," *IEEE Transactions on Smart Grid*, vol. 4, no. 1, pp. 479–488, 2013.

[54] S. Mirjalili, A. H. Gandomi, S. Z. Mirjalili, S. Saremi, H. Faris, and S. M. Mirjalili, "Salp Swarm algorithm: a bio-inspired optimizer for engineering design problems," *Advances in Engineering Software*, vol. 114, no. 6, pp. 163–191, 2017.

[55] M. Eusuff, K. Lansey, and F. Pasha, "Shuffled frog-leaping algorithm: a memetic meta-heuristic for discrete optimization," *Engineering Optimization*, vol. 38, no. 2, pp. 129–154, 2006.

[56] S. Daraban, D. Petreus, and C. Morel, "A novel MPPT (maximum power point tracking) algorithm based on a modified genetic algorithm specialized on tracking the global maximum power point in photovoltaic systems affected by partial shading," *Energy*, vol. 74, no. 5, pp. 374–388, 2014.

[57] M. M. Eusuff and K. E. Lansey, "Optimization of water distribution network design using the shuffled frog leaping algorithm," *Journal of Water Resources Planning and Management*, vol. 129, no. 3, pp. 210–225, 2003.